NeuroImage: Clinical 37 (2023) 103336

Contents lists available at ScienceDirect

NeuroImage: Clinical

journal homepage: www.elsevier.com/locate/ynicl

Atypical cortical processing of bottom-up speech binding cues in children with autism spectrum disorders

Jussi Alho [a,c,*], Sheraz Khan [a,b,c], Fahimeh Mamashli [a,b,c], Tyler K. Perrachione [e], Ainsley Losh [a], Nicole M. McGuiggan [a], Steven Graham [a], Zein Nayal [a], Robert M. Joseph [f], Matti S. Hämäläinen [b,c], Hari Bharadwaj [a,d,1], Tal Kenet [a,c,1,*]

[a] Department of Neurology, Massachusetts General Hospital, Harvard Medical School, 149 13th St, Boston, MA 02129, USA
[b] Department of Radiology, Massachusetts General Hospital, Harvard Medical School, 149 13th St, Boston, MA 02129, USA
[c] Athinoula A. Martinos Center for Biomedical Imaging, Massachusetts General Hospital, Harvard Medical School, 149 13th St, Boston, MA 02129, USA
[d] Department of Speech, Language, and Hearing Sciences, and Weldon School of Biomedical Engineering, Purdue University, 715 Clinic Drive, West Lafayette, IN 47907, USA
[e] Department of Speech, Language, and Hearing Sciences, Boston University, 635 Commonwealth Ave, Boston, MA 02215, USA
[f] Department of Anatomy and Neurobiology, Boston University School of Medicine, 72 East Concord St, Boston, MA 02118, USA

ARTICLE INFO

Keywords:
Autism
Speech
Magnetoencephalography
Functional connectivity
Phase-amplitude coupling

ABSTRACT

Individuals with autism spectrum disorder (ASD) commonly display speech processing abnormalities. Binding of acoustic features of speech distributed across different frequencies into coherent speech objects is fundamental in speech perception. Here, we tested the hypothesis that the cortical processing of bottom-up acoustic cues for speech binding may be anomalous in ASD. We recorded magnetoencephalography while ASD children (ages 7–17) and typically developing peers heard sentences of sine-wave speech (SWS) and modulated SWS (MSS) where binding cues were restored through increased temporal coherence of the acoustic components and the introduction of harmonicity. The ASD group showed increased long-range feedforward functional connectivity from left auditory to parietal cortex with concurrent decreased local functional connectivity within the parietal region during MSS relative to SWS. As the parietal region has been implicated in auditory object binding, our findings support our hypothesis of atypical bottom-up speech binding in ASD. Furthermore, the long-range functional connectivity correlated with behaviorally measured auditory processing abnormalities, confirming the relevance of these atypical cortical signatures to the ASD phenotype. Lastly, the group difference in the local functional connectivity was driven by the youngest participants, suggesting that impaired speech binding in ASD might be ameliorated upon entering adolescence.

1. Introduction

Autism spectrum disorder (ASD) is defined by deficits in social interactions and communication, and repetitive and restrictive behaviors. Individuals with ASD also commonly display a wide range of auditory processing abnormalities (Alcántara et al., 2004; Ben-Sasson et al., 2009; Bonnel et al., 2003; Kwakye et al., 2011; McCormick et al., 2016; O'Connor, 2012; Tomchek and Dunn, 2007). Neural manifestations of atypical auditory processing in ASD run the gamut from delayed evoked response latencies to simple tones (Edgar et al., 2015; Roberts et al., 2010) and single vowels (Oram Cardy et al., 2005; Roberts et al., 2011) all the way to abnormal cortical processing of spoken speech sentences (Alho et al., 2021). Gaining a better understanding of auditory processing of speech in ASD is of particular importance as early speech and language ability in children with ASD has been shown to predict adaptive functioning, social skills, and communicative abilities later in life

Abbreviations: ADOS, Autism Diagnostic Observation Schedule; ASD, autism spectrum disorder; ASPS, Auditory Sensory Profile Score; ERF, event-related field; ICSS, Inhibition Contrast Scaled Score; MSS, modulated sinewave speech; NVIQ, nonverbal IQ; PAC, phase-amplitude coupling; SCQ, Social Communication Questionnaire lifetime score; SCSS, Switching Contrast Scaled Score; SRS, Social Responsiveness Scale total score; SWS, sinewave speech; TD, typically developing; VIQ, verbal IQ.

* Corresponding authors.
E-mail addresses: jalho@mgh.harvard.edu (J. Alho), tal.kenet@mgh.harvard.edu (T. Kenet).

[1] These authors contributed equally as senior authors.

https://doi.org/10.1016/j.nicl.2023.103336
Received 13 June 2022; Received in revised form 10 January 2023; Accepted 20 January 2023
Available online 22 January 2023

(Howlin et al., 2004; Magiati et al., 2014).

A fundamental process in auditory perception is auditory scene analysis, whereby the brain organizes auditory information into coherent, perceptually meaningful objects or streams (Bregman, 1994). Spoken language, in particular, is a highly complex signal containing diverse and transient acoustic events, yet it is typically perceived as a single, coherent perceptual stream. It is thought that the brain achieves this kind of binding of different stimulus features into coherent perceptual objects through synchrony of the firing patterns of the neural populations that encode those features (Shamma et al., 2011). Dysfunction in this temporal synthesis of sensory information has been hypothesized to contribute to auditory processing abnormalities in ASD (Robertson and Baron-Cohen, 2017).

In a recent study, we used magnetoencephalography (MEG) to record cortical responses from children with ASD during a novel paradigm where perceptual binding of acoustic features of the stimulus into auditory objects was facilitated by manipulating the temporal coherence in the auditory scene with synthetic sounds (Bharadwaj et al., 2022). We found that the auditory cortical responses in children with ASD showed impaired sensitivity to increasing temporal coherence in the auditory scene, the extent of which correlated with behavioral measures of ASD severity and auditory processing abnormalities, suggesting that auditory scene analysis based on temporal coherence might indeed be impaired and contribute to auditory perceptual deficits in ASD. Given the importance of temporal coherence as a binding cue in natural sounds, the question arises as to whether such atypical processing of binding cues in ASD could also contribute to impaired speech processing.

At the neural level, abnormalities in temporal-coherence-based speech binding can be assessed by analyzing the synchrony of neural oscillations, which is believed to enable information transfer in the brain between neural populations (Fries, 2005). Many neuroimaging studies using a variety of paradigms have reported abnormalities in this information transfer mechanism in ASD, measured as long-range functional connectivity between disparate cortical regions and/or local functional connectivity within a functionally defined cortical region (Kana et al., 2014, 2011; Khan et al., 2013; Mamashli et al., 2021, 2018,2017; Nomi and Uddin, 2015; O'Reilly et al., 2017). Earlier studies from our group have documented reduced local functional connectivity in ASD using different analytic approaches and paradigms (Khan et al., 2015, 2013), suggesting that reduced local functional connectivity within a functionally relevant brain region might be characteristic of ASD. A commonly used analytical approach to study local functional connectivity is phase-amplitude coupling (PAC), whereby the phase of lower frequency oscillatory activity modulates the amplitude of higher frequency oscillatory activity (Canolty and Knight, 2010). For example, MEG studies using visual stimuli have reported decreased alpha (~8–12 Hz) to gamma (>30 Hz) PAC in ASD (Khan et al., 2013; Mamashli et al., 2018; Seymour et al., 2019). In parallel, ASD has been associated with atypically increased bottom-up processing tendencies (Amso et al., 2014; Järvinen-Pasley et al., 2008; Robertson et al., 2014). Thus, an important consideration when analyzing long-range functional connectivity in ASD is the directionality of the connectivity. It has been proposed that ASD could be characterized by increased long-range feedforward (i.e., bottom-up from previous stage in the processing hierarchy) and reduced long-range feedback (i.e., top-down from following stage in the processing hierarchy) connectivity (Khan et al., 2015; Kitzbichler et al., 2015).

Cortical processing of complex sounds is thought to occur hierarchically starting from representations of individual acoustic features in the primary auditory cortex to increasingly integrated representations that mirror object perception in higher cortical regions (Bizley and Cohen, 2013; Kaas and Hackett, 2000; Rauschecker, 1997; Rauschecker and Tian, 2000). Recent single-neuron and neuroimaging studies have suggested that parietal cortex might be a site where integrated representations of a coherent whole emerge from the elemental representations in the auditory cortex (Sohoglu et al., 2020; Yao et al., 2020).

Here, we directly investigated whether the brain functional connectivity correlates of binding the acoustic components of speech into a coherent perceptual stream are atypical in ASD. To this end, we recorded MEG while children with ASD (ages 7–17) and typically developing (TD) peers passively listened to three-tone sine-wave speech (SWS) sentences which only contain three time-varying sinusoidal components corresponding to the first three formant frequencies of the original speech sentences. Crucially, while SWS can be perceived as speech and understood by individuals who have already heard the intact original speech, they are perceived as set of simultaneous whistles by naïve listeners (Remez et al., 1981), because perceptual binding of these stimuli occurs purely through top-down influences (Davis and Johnsrude, 2007). Here, we compared MEG responses to these SWS stimuli to responses obtained when the same SWS sentences were amplitude modulated. Unlike the SWS sentences which lack bottom-up binding cues, the modulated SWS (MSS) sentences include both co-modulation (i.e., temporally coherent formant modulations) and a harmonic spectral structure, both of which are strong bottom-up grouping cues (Darwin, 1997). This contrast allows us to focus specifically on the cortical correlates of bottom-up speech binding in ASD. Based on studies of the cortical correlates of auditory object binding (Sohoglu et al., 2020; Yao et al., 2020) and the proposed increased long-range feedforward processing tendencies in ASD (Khan et al., 2015; Kitzbichler et al., 2015), we hypothesized that the ASD children would exhibit atypically increased feedforward functional connectivity (i.e., lack of selectivity in feedforward coherence-dependent routing) from primary auditory cortex to parietal cortex during the modulated SWS relative to the original SWS. Furthermore, based on our recent findings (Bharadwaj et al., 2022) and those suggesting that reduced local functional connectivity within a functionally relevant brain region might be characteristic of ASD (Khan et al., 2015, 2013; Mamashli et al., 2018; Seymour et al., 2019), we also hypothesized that binding the acoustic components of the modulated SWS would be impaired in the ASD children, and that this would manifest as decreased PAC in the parietal cortex. We tested these hypotheses by comparing data from children with ASD (N = 27) with age- and IQ-matched TD children (N = 28).

2. Material and methods

2.1. Participants

In total, 31 individuals between ages 7 to 17 who were previously diagnosed with autism spectrum disorder (ASD), and 35 age-matched typically developing (TD) individuals participated in the study. One potential ASD participant was excluded due to ultimately not meeting ASD criteria upon further evaluation. Five individuals (two ASD and three TD) were excluded from the analyses due to poor data quality. To match the resulting groups on nonverbal IQ (NVIQ), another five (one ASD and four TD) were excluded, resulting in a final sample of 27 ASD and 28 TD participants. Sample characteristics are summarized in Table 1 (for histogram of age distribution of the sample, see Supplementary Fig. S1).

All participants had normal hearing and confirmed hearing the stimuli well in each ear prior to the onset of the paradigm. Additionally, in all but nine participants (two TD and seven ASD), hearing was screened on the day of the experiment just prior to the session by examining whether otoacoustic emissions were present at octave frequencies from 500 Hz to 8000 Hz for primary levels of 50 and 60 dB SPL. One participant (ASD) was left-handed. Participants with ASD had a prior clinical diagnosis of ASD, which was further verified using the Autism Diagnostic Observation Schedule (ADOS; Lord et al., 2000) administered by trained research personnel who had established inter-rater reliability, and through the Social Communication Questionnaire, Lifetime Version. All ASD participants met criteria on the ADOS, and all but three met the cutoff (score > 15) on the SCQ. For the three participants that did not meet the cutoff on the SCQ, expert clinical

Table 1
Characterization of the participants. The p-values are from two-sample t-tests (two-tailed) for the difference in means between the ASD and TD groups. NVIQ: Nonverbal IQ; VIQ: Verbal IQ; ASPS: Auditory Sensory Profile Score; ICSS: NEPSY-II Inhibition Contrast Scaled Score; SCSS: NEPSY-II Switching Contrast Scaled Score; SCQ: Social Communication Questionnaire lifetime score; SRS: Social Responsiveness Scale total score; ADOS: Autism Diagnostic Observation Schedule score.

	ASD (N = 27, 4 females)			**TD** (N = 28, 6 females)			
	N	**mean (SD)**	**range**	**N**	**mean (SD)**	**range**	**p-value**
Age	27	14.0 (3.0)	7–17	28	13.6 (3.0)	7–17	0.67
NVIQ	27	104.9 (13.2)	74–136	28	110.3 (11.1)	93–130	0.11
VIQ	27	101.3 (16.7)	61–131	28	111.8 (14.2)	71–140	0.02
ADOS	27	11.3 (3.1)	5–17	–	–	–	–
SCQ	25	17.4 (6.6)	5–31	26	3.8 (3.3)	0–12	< 0.001
SRS	26	77.6 (10.6)	48–90	–	–	–	–
ASPS	25	16.4 (4.0)	7–24	27	22.6 (2.2)	18–25	< 0.001
ICSS	23	8.2 (3.6)	2–15	22	10.5 (3.8)	3–17	0.04
SCSS	23	9.0 (2.9)	1–14	21	10.0 (3.5)	4–17	0.33

impression (by R.M.J.) was used to determine inclusion (Risi et al., 2006). Individuals with autism-related medical conditions (e.g., Fragile-X syndrome, tuberous sclerosis) and other known risk factors (e.g., gestation < 36 weeks) were excluded from the study.

All TD participants were below threshold on the Social Communication Questionnaire and were confirmed to be free of any neurological or psychiatric conditions, and of substance use for the past 6 months, via parent-reports and self-reports. Verbal IQ (VIQ) and NVIQ were assessed with the Kaufman Brief Intelligence Test – II (Kaufman, 2004) for 22 ASD and 17 TD participants, and with the Differential Ability Scales – II (Elliot, 2007) for 5 ASD and 11 TD participants. Handedness information was collected using the Dean Questionnaire (Piro, 1998). The Social Responsiveness Scale parent report (SRS-2; Constantino and Gruber, 2012), which was designed as a quantitative measure of autism-related symptoms, was collected from all participants.

Additionally, Sensory Profile Questionnaire (Brown and Dunn, 2002) data were collected for 25 ASD and 27 TD participants. For the correlations between MEG data and behavioral scores, we focused specifically on the sum score of the first five questions of the Auditory section of the Sensory Profile (parent report), referred hereon as ASPS (Auditory Sensory Profile Score). The first five question measure auditory processing abnormalities in terms of sensitivity to and distraction by noise, and are categorically different from question 6–8, which are related to ignoring what parents say and not responding to name being called (question 6 and 7) and enjoying or seeking to make strange noises (question 8).

Lastly, a subset of participants completed the INN (Inhibition-Naming), INI (Inhibition-Inhibition), and INS (Inhibition-Switching) sections of the NEPSY-II evaluation. Derived from these sections, the Inhibition Contrast Scaled Score (ICSS) measures inhibition of attention, and the Switching Contrast Scaled Score (SCSS) measures attentional switching. The ICSS and SCSS scores range from 1 to 19. All research was in compliance with the Massachusetts General Hospital Institutional Review Board (MGH IRB), and all participants were consented in accordance with the Declaration of Helsinki and the approved protocol. Parents provided informed consent according to protocols approved by the MGH IRB.

2.2. Stimuli and paradigm

A sinewave speech sentence and its amplitude-modulated counterpart were used as stimuli (Fig. 1). The sinewave speech stimulus (SWS) was derived from a meaningless Jabberwocky sentence by extracting sinewave replicas of the first three formants through fitting an all-pole (autoregressive) linear predictive code filter (Ellis, 2004). The Jabberwocky sentence ("*Fu ðaki haɪn nʊl æk lə* tan") was taken from a corpus (Perrachione et al., 2015) and was created by re-arranging the phonemes of a phonetically rich English sentence ("*The tiny girl took off her hat*") while adhering to the phonotactic rules of English. The English sentence was taken from the IEEE sentences (IEEE, 1969). The English and Jabberwocky sentences were produced by a highly trained phonetician (T.K.P).

The modulated sinewave speech stimulus (MSS) was derived by amplitude modulating the SWS at 107 Hz. Importantly, while the 107 Hz

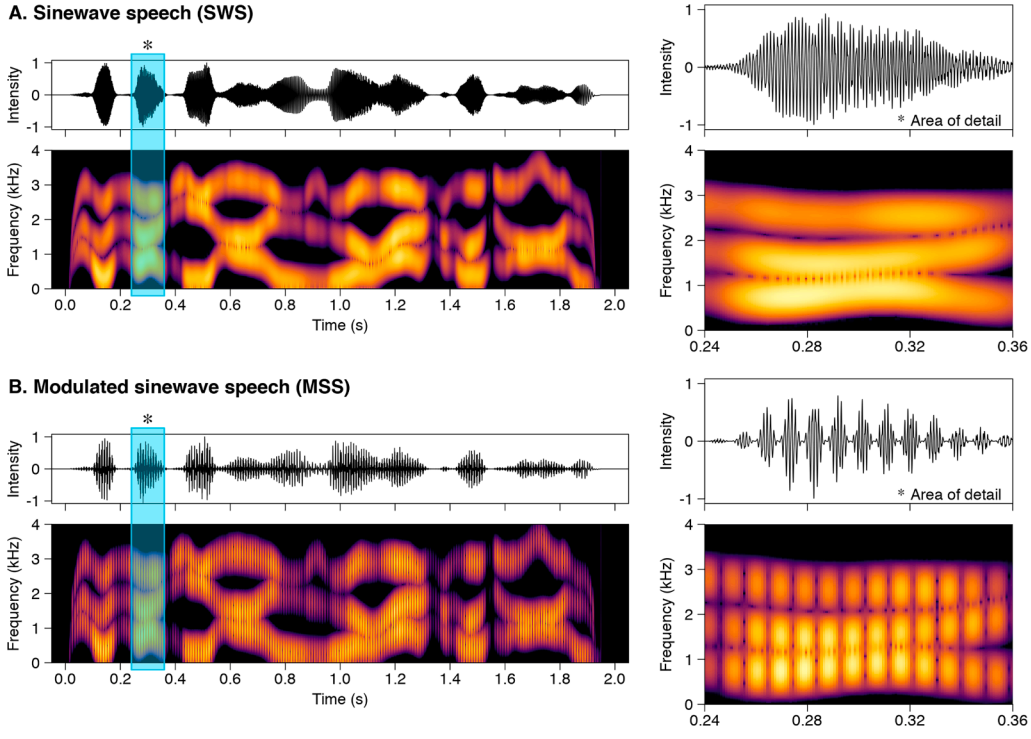

Fig. 1. Stimuli. Waveforms and spectrograms showing the acoustic differences between (A) sinewave speech (SWS) and (B) modulated sinewave speech (MSS). The * and light blue boxes highlight the areas of detail in the two stimulus types, shown at right. Note the presence of temporal modulation in the MSS stimuli evident in both the waveform and spectrogram, which facilitates perceptual binding of the three frequency components into a coherent auditory object. (For interpretation of the references to colour in this figure legend, the reader is referred to the web version of this article.)

modulation introduces both co-modulation of the formant components (i.e., temporal coherence in the amplitude fluctuations of the formant components) and harmonicity (and associated pitch) from the imposed modulations, which are strong bottom-up speech binding cues, it does not add any phonetic content derived from the intact (jabberwocky) speech.

In natural speech, both voicing (which produces co-modulation and harmonicity in the pitch range) and common onsets at the syllabic level provide temporal coherence across the speech components. However, in natural speech, voicing can also convey speech content and not just grouping cues (Rosen, 1992). By imposing modulations (at 107 Hz) in the pitch range, but unrelated to the voicing in the original speech, our design allowed us to study the effects of co-modulations and harmonicity on grouping *per se* dissociated from any phonetic content they may otherwise carry.

Previous work has shown that MSS is more intelligible than SWS in both children and adults (Lewis and Carrell, 2007). Furthermore, by imposing uncorrelated modulations on the different formants (rather than co-modulation), Carrell and Opie (1992) showed that the temporal coherence across the components (and not just that modulations are provided) is important in yielding improved speech intelligibility. See Supplementary material for audio files of the SWS and MSS stimuli as well as the Jabberwocky sentence from which the SWS and MSS were derived.

The stimuli were presented binaurally through insert earphones (Etymotic, Elk Grove Village, IL) at 75 dB sound pressure level. To ensure reliable and comparable responses regardless of the ability of the participant to maintain attention during the paradigm, the participants were watching a movie with the sound off and were instructed to ignore the sound stimuli. For most participants, both SWS and MSS stimuli were presented 60 times in the paradigm (for the exact participant-wise counts, see Supplementary Fig. S2). The stimuli were presented in random order with a 700–800 ms randomly varying inter-stimulus interval. The paradigm was presented in three runs, each lasting about 6 min. In addition to the SWS and MSS stimuli, the paradigm included two English speech sentences, two jabberwocky speech sentences, and two noise stimuli, not discussed here.

2.3. Structural MRI data acquisition and processing

T1-weighted magnetization-prepared rapid gradient echo (MPRAGE) structural images were acquired using a 3 T Siemens Trio MRI scanner (Siemens Medical Systems, Erlangen, Germany) and a 32-channel head coil (in-plane resolution 1x1 mm; slice thickness 1.3 mm, TR 2530 ms; TI 1100 ms; TE 3.39 ms; flip angle 7°). Cortical reconstructions and parcellations were generated using the FreeSurfer software (Version 6.0.0; documented and available at https://surfer.nmr.mgh.harvard.edu/).

2.4. MEG data acquisition

The MEG data were acquired with a whole-head 306-channel VectorView neuromagnetometer (MEGIN Oy, Finland) inside a magnetically shielded room (IMEDCO, Switzerland). The channels of this instrument are arranged in 102 sensor triplets with two orthogonal planar gradiometers and one magnetometer. The signals were band-pass filtered at 0.1–200 Hz prior to sampling at 1000 Hz. The position of the head was continuously recorded during the data acquisition using four head position indicator (HPI) coils attached to the scalp (Uutela et al., 2001). Locations of the HPI coils, three anatomical landmarks (nasion and auricular points), and multiple additional scalp surface points were digitized using a Fastrak digitizer (Polhemus) to allow coregistering the MEG and MRI data. Electrocardiography (ECG) and electro-oculography (EOG) signals were recorded to detect heartbeats, eye movements, and eye blinks. Additionally, 5 min of data were recorded without the subject present at the end of each session to estimate the noise covariance matrix for MEG source analysis.

2.5. MEG data preprocessing

Bad MEG channels were first detected using visual inspection. To compensate for head movements during the recording, and to reduce artifacts originating both from external sources outside the MEG sensor array and from the space between the brain and the MEG sensor array, we applied temporal Signal Space Separation (tSSS; Taulu and Kajola, 2005; Taulu and Simola, 2006) as implemented in the MNE-Python Maxwell filtering routine. The head movement (mean ± standard deviation) for the TD and ASD groups were 0.16 ± 0.11 mm and 0.25 ± 0.25 mm, respectively, with no significant difference between the groups (two-sample *t*-test: $t = 1.6$, $p = 0.11$). The head movements were quantified by converting the six head motion parameters (three translation and three rotation) to millimeters and combining them into a time series of head movement (by taking the Euclidean norm at each sample). The default parameters were used (inside expansion order of 8, outside expansion order of 3, subspace correlation limit of 0.98, and raw data buffer length of 10 s). Fine calibration and cross talk correction data specific to the recording site were applied.

Independent component analysis (ICA) was applied to the tSSS-processed data to reduce systematic physiological artifacts, such as eye blinks and heartbeats. More specifically, FastICA (Hyvärinen, 1999) was used to decompose MEG signals into maximally independent components (ICs). The ICA decomposition was estimated on band-pass filtered (1 Hz highpass, 40 Hz lowpass) data. Segments where signal amplitude exceeded 4000 fT/cm and 4000 fT on the gradiometers and magnetometers, respectively, were excluded from the estimation. The ICs corresponding to ECG or EOG activity were identified based on Pearson correlation and visual inspection of scalp topographies corresponding to each of the components. The number of ICs rejected from the data (mean ± standard deviation) in the TD and ASD groups were 3.12 ± 0.42 and 3.17 ± 0.49, respectively.

2.6. Source estimation

The cortical surface reconstruction provided by FreeSurfer was decimated by recursively subdividing the faces of an octahedron six times for both hemispheres, leading to a grid of 4098 dipoles per hemisphere. The forward solution was computed using a single-compartment boundary-element model (Hämäläinen and Sarvas, 1987). The inner skull surface triangulations were generated from the MRI data using the watershed algorithm. The cortical current distribution was estimated using minimum-norm estimate (MNE) solution (Hämäläinen and Ilmoniemi, 1994) by fixing the source orientation perpendicular to the cortex and using depth weighting (Lin et al., 2006) of 0.8. For the delineation of the auditory cortical regions-of-interest (ROIs), noise-normalized dynamic statistical parametric mapping (dSPM) estimates (Dale et al., 2000) were used. The noise covariance matrix used in the inverse operator was estimated from the empty room data.

2.7. Delineating primary auditory cortex

To delineate primary auditory cortex (A1), we first identified the superior and transverse temporal gyri using the individual FreeSurfer cortical parcellation (Desikan et al., 2006). In this anatomical region, we defined the peak amplitude of activation within the first 500 ms after stimulus onset based on the dSPM estimates of the evoked responses derived by averaging epochs across the SWS and MSS conditions. The dSPM estimate gives a test statistic of the signal-to-noise ratio of MNE and therefore allows the delineation of the areas of activity with high signal-to-noise ratio. Before averaging, the epochs were low-pass filtered at 30 Hz, baseline-corrected using a 200-ms prestimulus period, and the epoch counts between the SWS and MSS conditions were equalized by

dropping epochs, so that the remaining SWS and MSS epochs occur as close as possible in time. At the latency of the peak amplitude of activation, we selected five dipoles with the highest dSPM values to be used as ROIs. This procedure was repeated for both cerebral hemispheres in each participant. Fig. 2 shows the overlapping probability of left and right A1 across participants visualized by morphing the ROIs onto the FreeSurfer average brain.

2.8. Auditory event-related fields

For each participant, we calculated event-related fields (ERFs) for the SWS and MSS conditions by averaging the epochs. Before averaging, the data were filtered at 1–30 Hz and baseline corrected by subtracting the mean amplitude in a 200-ms pre-stimulus period from the signals. In case the epoch counts for SWS and MSS were not equal, they were equalized before averaging by dropping epochs so that the remaining SWS and MSS epochs occur as close as possible in time. ERFs for left and right A1 were then obtained by averaging the MNE source estimates across the vertices within the regions. To avoid signal cancellations, the polarity of time courses at vertices whose orientation was>90° relative to the dominant direction were flipped before averaging.

2.9. Seed-based functional connectivity

We computed seed-based functional connectivity separately from left and right A1 to the rest of the cortex. To this end, we first averaged the source time courses across the vertices within left and right A1 using sign flips when necessary (as described in section 2.8). Time-frequency decomposition of the resulting mean time courses of left and right A1 and time courses of the rest of the cortical vertices was done using convolution with complex Morlet wavelets (each spanning seven cycles) in a frequency range of 4–60 Hz and a time window of −500–1500 ms with respect to stimulus onset. Connectivity was quantified as the consistency of phase synchrony across epochs between the sources (i.e., A1 and a given vertex) for every time and frequency point using debiased squared weighted phase lag index (WPLI) (Vinck et al., 2011).

We chose WPLI as the connectivity metric for its robustness against spurious connectivity caused by MEG field spread. That is, it can be assumed that non-zero phase lag between time courses is not caused by field spread from a common source but rather by true connectivity between brain regions via a physical medium, which is bound to have a delay (i.e., non-zero phase lag). In WPLI, non-zero phase lag interdependencies are estimated by weighting the contribution of observed phase leads and lags by the magnitude of the imaginary component of the cross-spectrum between each pair of time courses. WPLI range from 0 to 1, with 0 indicating random distribution of phase and 1 indicating constant (non-zero lag) phase difference across epochs. As the number of epochs available varied between the participants (see Supplementary Fig. S2), we chose to use the debiased squared version of the WPLI which accounts for sample-size bias.

The results for each frequency were first binned into theta (4–8 Hz), alpha (8–12 Hz), beta (12–30 Hz), and gamma (30–60 Hz) bands, and then averaged within the time window and each frequency band to obtain a mean connectivity value for each vertex, condition, and participant. Before the connectivity computation, the epoch counts were equalized between the SWS and MSS conditions within participant by dropping epochs so that the remaining SWS and MSS epochs occur as close as possible in time. The analysis was performed using MNE-Python (Version 0.24.0; Gramfort et al., 2013).

We used cluster-based permutation statistics (Maris and Oostenveld, 2007) to determine cortical regions of significant group difference. To this end, the data of each participant was first morphed to a FreeSurfer average cortical representation (Fischl et al., 1999). We excluded the medial wall, limbic lobe, and occipital lobe from the analysis and ran the test separately for the left and right hemispheres (as there are no interhemispheric spatial-adjacency-based clusters) using an F-test (two-tailed) with cluster-defining threshold of $F = 2.78$ (corresponding to $p = 0.01$) and 5000 permutations. Cluster-level statistics were calculated by summing the *t*-statistics within the defined cluster. Multiple comparisons corrected p-value for each cluster was calculated as the proportion of permutation runs with random partitions where the cluster statistic was greater than or equal to the cluster statistic for the difference between the original groups. The null hypothesis of no difference between the groups was rejected at $p < 0.05$. Normalization of the SWS and MSS relative to baseline (SWS-BL and MSS-BL) conditions was done by first averaging the mean connectivity during the baseline period (-500–0 ms) of SWS and MSS stimuli and subtracting the resulting average from the connectivity during the SWS and MSS stimuli (calculated as the mean across the 0–1500 ms post-stimulus period). Normalization of the MSS relative to SWS (MSS-SWS) condition was done by subtracting the connectivity during the SWS stimulus from the connectivity during the MSS stimulus. Post-hoc group differences in a significant cluster were tested using Wilcoxon rank-sum test (quantified by z and p-value) with the corresponding effect sizes determined using rank-biserial correlation (r_b). For the correlation calculations, we selected the peak connectivity value for each participant within the cluster showing significant group difference. Differences in correlations between groups were assessed using Fisher's r-to-z transformation.

2.10. Directionality of the functional connectivity

To estimate directionality of the functional connectivity, we computed nonparametric Granger causality (Dhamala et al., 2008a, 2008b) between time courses extracted from the seed A1 and the cortical cluster showing significant group difference. We selected 10 vertices with the highest statistic values within the cluster and morphed the

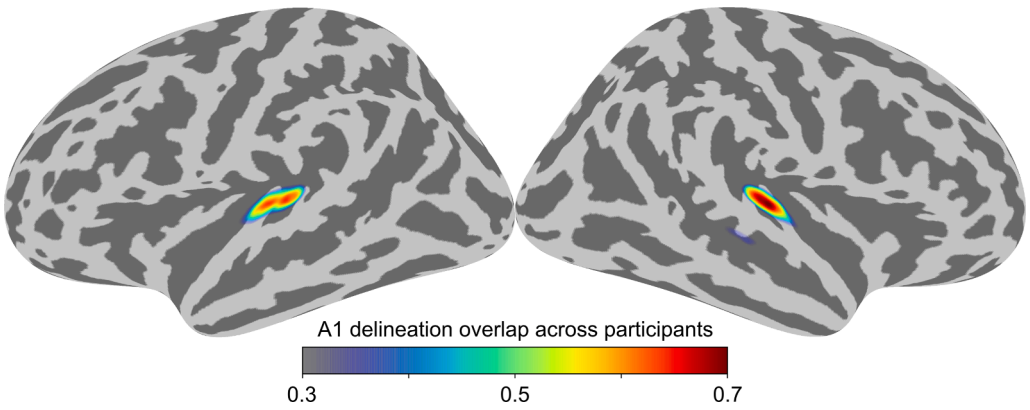

Fig. 2. Functional regions-of-interest (ROIs). Probability map of left and right A1 delineation overlap across participants (N = 55).

vertices to each participant's individual cortical surface. Both time courses were then extracted by averaging the vertex time courses and using sign flips when necessary to avoid signal cancellations (as described in section 2.8).

For the estimation of feedforward functional connectivity, we used multitaper frequency transformation for 4–60 Hz with 2 Hz steps based on discrete prolate spheroidal (Slepian) sequences (3 tapers, ±4 Hz smoothing) of the epoched time courses using a 500-ms sliding window for 0–1500 ms with 100 ms steps following stimulus onset and computed the Granger causality scores for each window using nonparametric spectral matrix factorization (Dhamala et al., 2008b). Normalization of the SWS and MSS relative to baseline (SWS-BL and MSS-BL) conditions was done by averaging the scores of the baseline period (-500–0 ms) of SWS and MSS and subtracting the average from the scores of the post-stimulus time windows of SWS and MSS. Normalization of the MSS relative to SWS (MSS-SWS) condition was done by subtracting the SWS scores from the MSS scores between the corresponding time windows. Additionally, we estimated the overall feedback functional connectivity by combining the SWS and MSS conditions and computing the nonparametric Granger causality between −500–1500 ms (using identical frequency analysis and sliding window parameters as for the feedforward connectivity estimation). Group differences in the Granger causality scores in the time–frequency domain were determined using cluster-based permutation statistics (Maris and Oostenveld, 2007). The nonparametric Granger causality analysis was performed using FieldTrip toolbox (Oostenveld et al., 2011).

2.11. Phase-amplitude coupling

To analyze local connectivity, we computed phase-amplitude coupling (PAC) between alpha band (8–12 Hz with 0.5 Hz steps) phase and gamma band (30–60 Hz with 3 Hz steps) amplitude for each vertex within the region showing significant group difference in functional connectivity between A1 and parietal lobe based on the seed-based functional connectivity analysis. Before epoching the data, the whole time courses were first band-pass filtered with 2 Hz bandwidth for the alpha band phase and with 24 Hz bandwidth (twice as high as the highest frequency for the phase) for the gamma band amplitude (for discussion on optimal filtering parameters in PAC analysis, see (Dupré la Tour et al., 2017)).

The instantaneous phase of the alpha and amplitude of the gamma frequencies were extracted using Hilbert transformation of the filtered time courses. Epochs between 0 and 1500 ms after stimulus onset were then extracted from the filtered and Hilbert transformed data for both the SWS and MSS conditions. To prevent spurious PAC due to sharp edges in the data, the epochs were concatenated into one vector per vertex (Kramer et al., 2008). Additionally, a baseline condition was created from the 500 ms prestimulus periods. To match the SWS and MSS conditions in total data duration, three times as many prestimulus periods as the number of epochs were used per participant. To quantify the degree of PAC, we used the normalized modulation index by Özkurt and Schnitzler (2011). The analysis was performed with the help of the pactools package (Dupré la Tour et al., 2017).

Cluster-based permutation statistics (Maris and Oostenveld, 2007) were used to determine regions of significant group difference (for the parameters, see section 2.9). For the correlation calculations, we selected the peak PAC value for each participant within the cluster showing significant group difference. Differences in correlations between groups were assessed using Fisher's r-to-z transformation. All analyses were performed with the help of the Massachusetts Life Sciences Center (MLSC) Compute Cluster.

2.12. Data and code availability

The MRI data were processed using the FreeSurfer software (Version 6.0.0; available at https://surfer.nmr.mgh.harvard.edu/ and https://github.com/freesurfer/freesurfer). The MEG data processing was done with the help of the MNE-Python software (Version 0.24.0; available at https://mne.tools/stable/index.html and https://github.com/mne-tools/mne-python). The phase-amplitude coupling analysis was performed with the help of the pactools package (available at https://github.com/pactools/pactools). All custom codes used in the processing and analyses of the data will be made available upon the acceptance of this paper (https://github.com/Kenet-lab). The raw behavioral, MEG, and MRI data supporting the conclusions of this article will be made available by the authors following approval of the required Massachusetts General Hospital Data Sharing agreement.

3. Results

3.1. Auditory event-related fields (ERFs)

We began by examining whether the auditory cortical activity elicited by the SWS and MSS stimuli differed between the groups. Supplementary Figure S3A and S3B show the ERFs during the 0–1500 ms window following stimulus onset in the left and right primary auditory cortex (A1) ROIs, respectively. We did not find any statistically significant group differences in the ERFs in the MSS relative to SWS (MSS-SWS) condition in either hemisphere (Supplementary Fig. S3C and S3D).

3.2. Group differences in seed-based functional connectivity

Next, to assess the hypothesis that ASD children would exhibit atypically increased feedforward functional connectivity from A1 to parietal cortex in MSS-SWS, we first investigated whether there were any group differences in the seed-based connectivity, using left and right A1 as separate seeds. A statistically significant difference was found for MSS-SWS at alpha band (8–12 Hz) with the left A1 as seed (cluster p-value = 0.003; Fig. 3A), mostly overlapping with the following regions of the FreeSurfer parcellation (Desikan et al., 2006): supramarginal (15 %), postcentral (45 %), and precentral (31 %), with the peak of the group difference within supramarginal. Post-hoc Wilcoxon rank-sum test on the mean WPLI values from the cluster revealed significantly stronger connectivity in ASD compared to TD for MSS-SWS ($z = 4.02$, $p = 0.00006$, $r_b = 0.63$) and for MSS relative to baseline (MSS-baseline; $z = 2.32$, $p = 0.02$, $r_b = 0.37$; Fig. 3B). For results from within-group tests on differences between MSS and SWS in the left A1 seed functional connectivity, see Supplementary Figure S4. No group differences were found with the right A1 as seed.

3.3. Directionality of the seed-based functional connectivity

Then, we tested whether the increased functional connectivity in the ASD group would indeed be feedforward as we hypothesized. Nonparametric Granger causality analysis revealed stronger feedforward functional connectivity from A1 to the parietal cortex in ASD compared to TD group within the first 500 ms following stimulus onset at alpha band (~8–12 Hz) for MSS-SWS (cluster p-value = 0.014, Wilcoxon rank-sum test using values within the cluster: $z = 3.65$, $p = 0.0003$; Fig. 4). We did not find any statistically significant group differences in the parietal cortex to A1 feedback functional connectivity (see Supplementary Fig. S5).

3.4. Group differences in phase-amplitude coupling (PAC)

Next, to test our hypothesis that binding the acoustic components of MSS would be impaired in the ASD children, we examined local functional connectivity using phase-amplitude coupling (PAC) within the parietal region that showed group difference in the long-range functional connectivity with left A1 (Fig. 5A, blue patch). We found a significant group difference in alpha (8–12 Hz) phase to gamma (30–60 Hz) amplitude coupling for MSS-SWS (cluster p-value = 0.024; Fig. 5A, red-

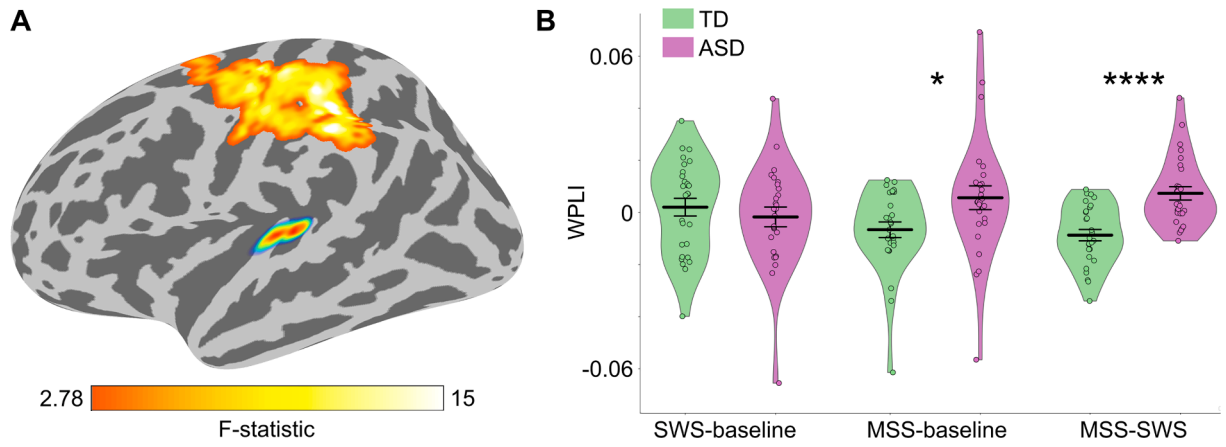

Fig. 3. Seed-based functional connectivity. (A) Cluster of significant seed-based connectivity (WPLI) group difference in MSS relative to SWS (MSS-SWS) at alpha band (8–12 Hz), with the seed (left A1) also shown. (B) Plots of group mean WPLI (thick horizontal black line) with kernel density estimation (KDE) of the underlying distributions for SWS-baseline, MSS-baseline, and MSS-SWS. Individual WPLI values are overlaid on the KDE plot. The WPLI values were derived by averaging values within the cluster in A. Error bars around the mean represent standard error of the mean. Statistically significant group differences in Wilcoxon rank-sum test are indicated by asterisks (*$p < 0.05$, ****$p < 0.0001$).

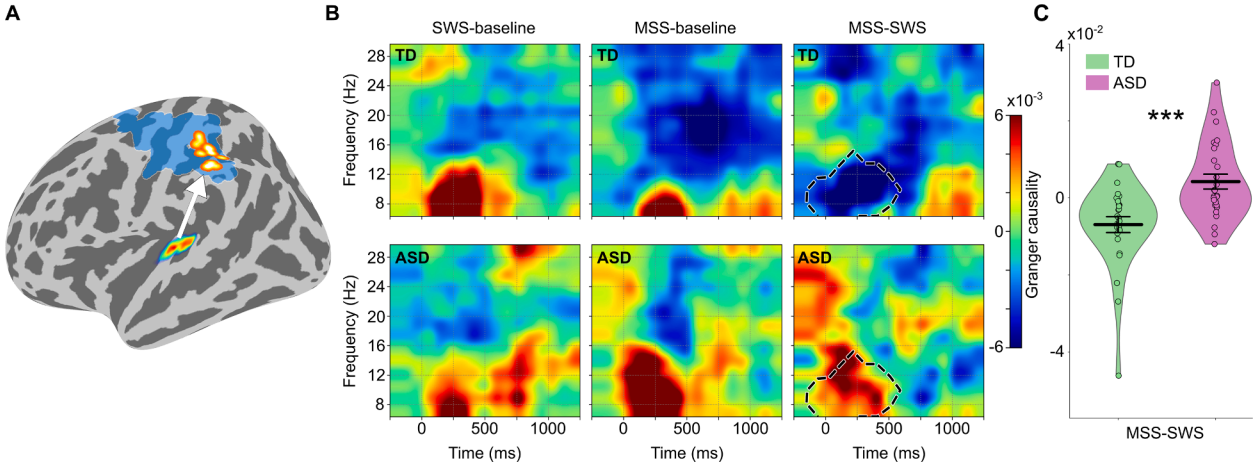

Fig. 4. Directionality of the functional connectivity. (A) Feedforward functional connectivity between the left A1 and the parietal area showing the strongest group difference in the MSS relative to SWS (MSS-SWS) functional connectivity (red-yellow cluster) estimated using nonparametric Granger causality. The blue area denotes the whole area of significant MSS-SWS group difference in the seed-based connectivity of the left A1 (see Fig. 3A). (B) Group mean Granger causality scores for SWS-baseline, MSS-baseline, and MSS-SWS in time–frequency domain with statistically significant group difference cluster outlined. The time axis indicates the center points of the 500 ms sliding windows from 0 to 1500 ms. (C) Group mean Granger causality scores (thick horizontal black line) within the MSS-SWS cluster in B (encircled with black dashed line) with kernel density estimation (KDE) of the underlying distributions for MSS-SWS. Individual scores are overlaid on the KDE plot. Error bars around the mean represent standard error of the mean. ***$p < 0.001$ in Wilcoxon rank-sum test. (For interpretation of the references to colour in this figure legend, the reader is referred to the web version of this article.)

yellow patch). Wilcoxon rank-sum test on the mean PAC values from the cluster revealed significantly weaker PAC in ASD compared to TD for the MSS-SWS ($z = 2.90$, $p = 0.004$, $r_b = 0.46$; Fig. 5B). To test the validity of our hypothesis, we conducted a post-hoc analysis by calculating PAC in the whole brain using the phase and amplitude frequency of the largest group difference in PAC within the found cluster (i.e., 10 Hz for phase and 45 Hz for amplitude; Fig. 5C). Fig. 5D shows that, after cluster correction, the only surviving clusters of significant PAC group difference were found within the ROI in the left parietal lobe (see also Supplementary Fig. S6).

3.5. Correlation between seed-based functional connectivity, directionality, and PAC

To determine the dependency between the different connectivity measures, we tested whether the seed-based functional connectivity correlated with the directionality or PAC measures. The seed-based functional connectivity between left A1 and the parietal region (that showed the strongest group difference; see Fig. 4A) correlated positively with the degree of "feedforwardness" (estimated by non-parametric Granger causality) in the ASD group in MSS-baseline ($r = 0.59$, $p = 0.001$; Supplementary Fig. S7A) and MSS-SWS ($r = 0.43$, $p = 0.03$; Supplementary Fig. S7B). In other words, the stronger the functional connectivity between left A1 and the parietal region, the stronger the feedforward drive between these regions in the ASD group. The within-group correlations between the seed-based functional connectivity and PAC (that showed significant group differences; see Fig. 5A) did not reach significance (Supplementary Fig. S7C, D).

3.6. Correlation between the functional connectivity measures and participant characteristics

Finally, to determine whether the atypical connectivity in the ASD group was related to any of the participants characteristics or traits, we

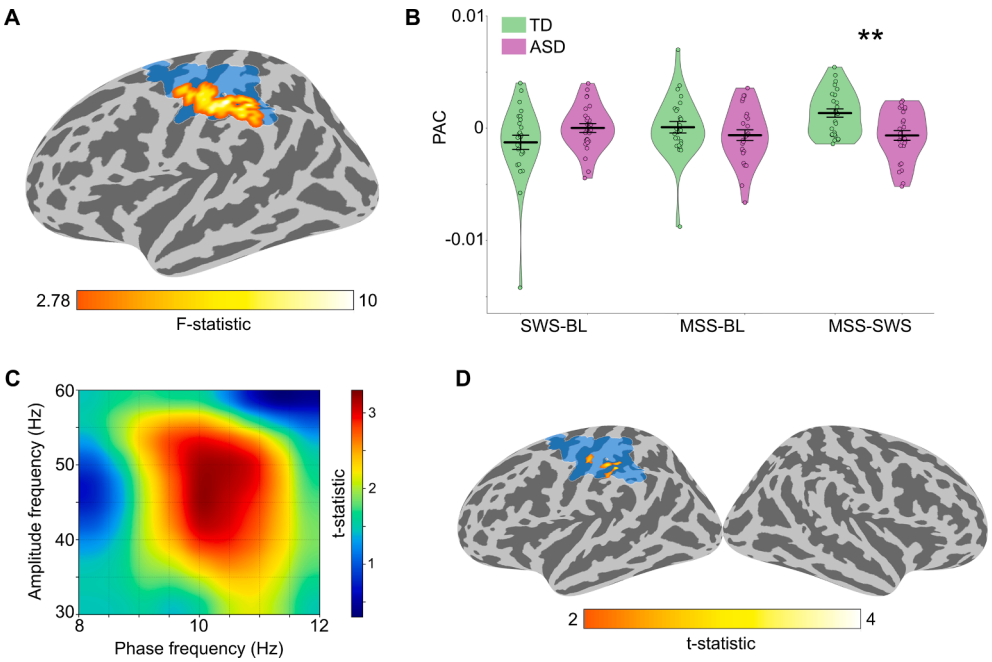

Figure 5. Phase-amplitude coupling (PAC). (A) Cluster of significant group difference in alpha phase (8–12 Hz) to gamma (30–60 Hz) amplitude coupling in the MSS relative to SWS condition (MSS-SWS). The blue area denotes the area of significant MSS-SWS group difference in the seed-based connectivity of the left A1 (see Fig. 3A). (B) Plots of group mean PAC (thick horizontal black line) with kernel density estimation (KDE) of the underlying distributions for the SWS-baseline, MSS-baseline, and MSS-SWS. Individual PAC values are overlaid on the KDE plot. The PAC values were derived by averaging values within the cluster in A. Error bars around the mean represent standard error of the mean. Statistically significant group differences in Wilcoxon rank-sum test are indicated by asterisks (**$p < 0.01$). (C) PAC group difference *t*-statistics in the MSS-SWS condition within the cluster in A. (D) PAC group difference *t*-statistics in the MSS-SWS condition in the whole cortex, calculated using the frequencies of the peak group difference determined from C (i.e., 10 Hz for phase and 45 Hz for amplitude) and thresholded at $p < 0.05$ (one-tailed) and cluster size > 10 vertices. For whole-cortex PAC group difference calculated using the full frequency range (i.e., alpha [8–12 Hz] phase to gamma [30–60 Hz] amplitude), see Supplementary Figure S6.

tested for correlations of the long-range functional connectivity values extracted from the cluster showing significant group difference in the seed-based connectivity of left A1 with age as well as behavioral scores. We did not find any significant correlations between the left A1 seed functional connectivity and age in either MSS-baseline (TD: r = 0.07, p = 0.72; ASD: r = 0.06, p = 0.75) or MSS-SWS (TD: r = -0.01, p = 0.94; ASD: r = -0.03, p = 0.88). Similarly, overall ASD severity, as measured by the SRS scores, did not correlate significantly with the left A1 seed functional connectivity in the ASD group (MSS-baseline: r = 0.13, p = 0.53; MSS-SWS: r = 0.16, p = 0.44).

We then examined whether we could predict abnormal auditory processing as measured behaviorally using the ASPS, where lower scores indicate more severe auditory processing abnormalities. We found a significant negative correlation between the connectivity and the ASPS in the ASD group in both MSS-baseline (r = -0.45, p = 0.024; Fig. 6A) and MSS-SWS (r = -0.42, p = 0.036; Fig. 6B). In other words, the more severe the auditory processing abnormalities, the stronger the connectivity between left A1 and the observed cluster in the parietal cortex in the ASD group was. Both correlations also differed significantly between the groups (MSS-baseline: z = 2.18, p = 0.029; MSS-SWS: z = 1.98, p = 0.047).

Similarly, we tested whether the weaker PAC in the ASD compared to TD group was associated with any participant characteristics. PAC in MSS-SWS condition and age of the participants showed negative

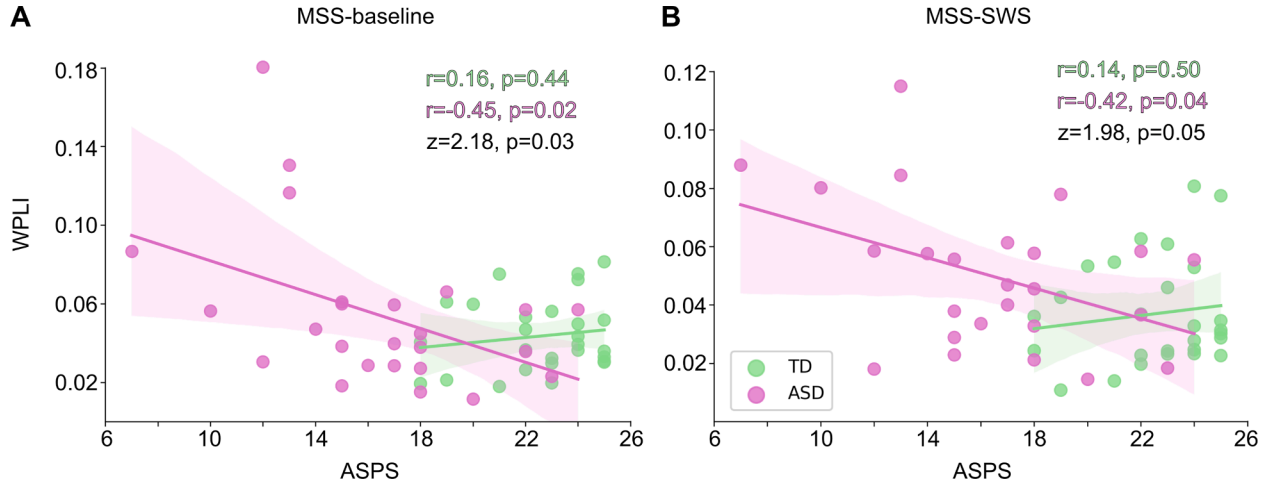

Fig. 6. Correlation between the seed-based functional connectivity and scores measuring auditory processing abnormalities (ASPS). Correlation between the ASPS scores and functional connectivity in (A) MSS-baseline and (B) MSS-SWS. The functional connectivity values were extracted from the cluster showing significant group difference in the seed-based connectivity of the left A1 (see Fig. 3A). The shaded areas (TD in green, ASD in purple) encompass the 95% confidence interval for the correlation. Correlation coefficients (r) and p-values for the within-group correlations, and z-scores and p-values for the difference between the within-group correlations are shown in the plots. (For interpretation of the references to colour in this figure legend, the reader is referred to the web version of this article.)

correlation in the TD group (r = -0.58, p = 0.001), with a significant difference between the within-group correlations (z = 3.12, p = 0.002; Fig. 7). There was no significant correlation between PAC and SRS scores measuring overall ASD severity (r = -0.16, p = 0.45), and unlike the finding with long-range functional connectivity, no significant correlation between PAC and ASPS either (TD: r = -0.36, p = 0.07; ASD: r = 0.13, p = 0.54).

We also tested for potential correlations between two behavioral scores measuring attentional inhibition (ICSS) and attentional switching (ICSS) and local and long-range functional connectivity measures. Neither of these behavioral measures of attention correlated significantly with either one of the functional connectivity measures, in either group.

4. Discussion

The aim of this study was to investigate neural deficits associated with the impaired processing of spoken language often documented in ASD. More specifically, we studied whether the cortical correlates of integrating speech-related acoustic features into a coherent speech stream were atypical in ASD. As hypothesized, our results showed that, relative to TD children, ASD children had greater long-range feedforward functional connectivity from left primary auditory cortex to parietal cortex during MSS relative to SWS. In parallel, the ASD group had decreased local functional connectivity within the left parietal cortical region during MSS relative to SWS, measured using phase-amplitude coupling. The increased long-range functional connectivity in the ASD group correlated with behavioral scores measuring auditory processing abnormalities. Lastly, decreased local connectivity in the ASD group was associated with different maturational trajectories between the groups, revealing that the group difference in local phase-amplitude coupling was driven by the youngest participants.

4.1. Increased feedforward functional connectivity in ASD

We found increased long-range functional connectivity in the ASD group for MSS relative to SWS between left primary auditory cortex (A1) and a region centered in left lateral parietal cortex (see Fig. 4). This region extended from the left temporoparietal junction to premotor cortex (Brodmann area 6), peaking in supramarginal gyrus (SMG; Brodmann area 40). These areas are linked to cortical speech processing as part of the dorsal auditory stream (Rauschecker and Scott, 2009). In addition to the known roles in spatial processing (Rauschecker and Tian, 2000) and sensorimotor integration (Hickok and Poeppel, 2007; Rauschecker, 2011), the dorsal auditory stream has more recently been proposed to engage in time-dependent sequence processing, including the segmentation and combination of increasingly larger linguistic chunks in time during sentence processing (Bornkessel-Schlesewsky and Schlesewsky, 2013). Such dynamic perception requires precise temporal processing and coherence-dependent analysis and selective routing of auditory information in speech (Giraud and Poeppel, 2012). Disruptions in the temporal synthesis of sensory signals have been suggested to characterize perceptual processing in ASD (Bharadwaj et al., 2022; Robertson and Baron-Cohen, 2017; Van Der Hallen et al., 2015).

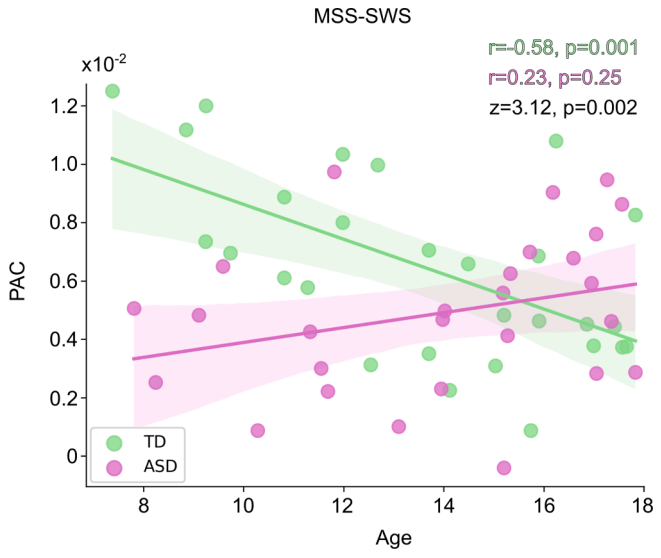

Fig. 7. Phase-amplitude coupling (PAC) maturational trajectories. Correlation between PAC and age in MSS-SWS. The PAC values were extracted from the cluster showing significant group difference (see Fig. 5A). The shaded areas (TD in green, ASD in purple) encompass the 95% confidence interval for the correlation. Correlation coefficients (r) and p-values for within-group correlations, and z-scores and p-values for the difference between the within-group correlations are shown in the plot. (For interpretation of the references to colour in this figure legend, the reader is referred to the web version of this article.)

Post-hoc Granger causality analysis revealed a significant group difference in the directionality of the connectivity with the ASD group showing increased A1 to SMG feedforward drive (see Fig. 5). Considering that the increased intelligibility of the MSS relative to SWS stimulus (due to the restored binding cues) enables the brain to rely more on bottom-up as opposed to top-down processes in the perception of this stimulus, the observed increased A1 to SMG feedforward connectivity in the ASD group is consistent with previous behavioral studies showing increased bottom-up processing tendencies in ASD (Amso et al., 2014; Järvinen-Pasley et al., 2008) as well as with the proposed abnormally increased feedforward connectivity in ASD (Bharadwaj et al., 2022; Khan et al., 2015; Kitzbichler et al., 2015; Mamashli et al., 2017), seemingly lacking the typical selectivity in the routing of sensory information in a coherence-dependent manner (Hull and Scanziani, 2007).

At the individual level, increased functional connectivity was associated with increased severity of auditory processing abnormalities in the ASD group (see Fig. 7). The correlation between connectivity and auditory processing abnormalities in the ASD group also differed significantly from that same correlation in the TD group, which trended in the opposite direction. This, together with the increased feedforward drive in the ASD group, suggests that abnormal speech processing in ASD may be driven at least in part by differences in low-level auditory processing, rather than resulting from modulation of auditory processing by higher-order cognitive mechanisms such as attention. Taken together, the increased feedforward functional connectivity from A1 to SMG for the more speech-like MSS relative to SWS stimuli in the ASD group could be interpreted as abnormal temporal processing and bottom-up binding of sentence-length speech stimuli in ASD, resulting from differences in low-level auditory processing and manifested as increased feedforward processing within the dorsal auditory stream.

4.2. Reduced local functional connectivity in ASD

In parallel with the increased A1 to SMG long-range connectivity, we found reduced local functional connectivity within SMG for MSS relative to SWS in the ASD group (see Fig. 6). Since the binding cues across the tones (representing formants) were eliminated in the SWS stimulus but restored in the MSS stimulus through increased temporal coherence and harmonicity, this finding implies that binding formants into intelligible speech might be abnormal in ASD, further supporting the interpretation of abnormal temporal processing in ASD. Such deficit could contribute also to well-documented higher-order language impairments in ASD (Arnett et al., 2018; Bloy et al., 2019; Lee et al., 2017; Lombardo et al., 2015). This finding also expands on our recent study where auditory cortical responses in ASD children showed insensitivity to increasing temporal coherence in the auditory scene (Bharadwaj et al., 2022) and is consistent with the temporal binding hypothesis of autism (Brock et al., 2002).

The cortical location of the significant group difference in local

functional connectivity is in agreement with findings from previous studies linking parietal cortex to binding representations of separate acoustic features into a coherent object (Sohoglu et al., 2020; Yao et al., 2020). For instance, in their recent study using fMRI and multivariate pattern analysis, Sohoglu et al. (Sohoglu et al., 2020) found integrated multivoxel representations of acoustic features in the left lateral parietal cortex around the inferior and superior parietal lobules whereas independent representations of the component acoustic features were found in the superior temporal plane around A1. In light of these findings, the parallel abnormalities in A1 to SMG long-range connectivity and in local connectivity within SMG in the ASD group are consistent with the interpretation of disruption to the integration of independent representations of acoustic components into a coherent whole.

The maturational trajectories of the local connectivity (PAC) measures were significantly different between the groups (see Fig. 7). In the TD group, a negative correlation was observed between the individual connectivity measures and age, indicating that the youngest TD participants had the strongest local connectivity. In contrast, the ASD group showed an opposite trend. In other words, the significant group difference in local connectivity was driven by participants below 14 years of age, implying that the proposed abnormality in auditory object binding in ASD might ameliorate with maturation.

These results are in line with previous findings of inverse maturational trajectories for auditory processing between TD and ASD groups (Alho et al., 2021; Edgar et al., 2015; Port et al., 2016; Stephen et al., 2017) and in PAC measures during visual processing of emotional faces (Mamashli et al., 2018). For example, using a subsample of the present study, we recently showed that the maturational trajectories of MEG-measured auditory cortical responses to natural speech sentences were similarly divergent between the TD and ASD groups: While the response strength decreased with age in the TD group (possibly reflecting increasingly efficient language processing through synaptic pruning (Changeux and Danchin, 1976), the opposite was observed in the ASD group (Alho et al., 2021). A similar interpretation could hold for the present findings. The opposite maturational trajectories could also relate to the relatively slow maturation of the dorsal auditory stream in language processing (Brauer et al., 2013; Zhang et al., 2007) which could make it more susceptible to disturbance during development, as has also been suggested for the dorsal visual stream (Braddick et al., 2003) in the context of a tentative dorsal visual stream deficiency in ASD (Grinter et al., 2010; Pellicano et al., 2005; Spencer et al., 2000).

Interestingly, identical maturational trajectories to those observed here have been documented in audiovisual integration of speech. For example, Foxe et al. (2015) showed that the deficits in integrating heard and seen speech that were evident in 5–12 year-old ASD children were fully ameliorated in 13–15 year-old ASD children. Similarly, a study on the perception of the McGurk effect in 7–16 year-old ASD children demonstrated an audiovisual integration deficit that diminished with age (Taylor et al., 2010). Even though multisensory (audiovisual) binding of heard and seen speech cues is a distinct from intramodal auditory binding of acoustic features of speech, both are thought to be mediated by temporal coherence. It is therefore possible that deficits in temporal coherence processing during speech perception could ameliorate during adolescence in ASD. There is also some evidence that the postulated dorsal visual stream deficiency in ASD, found using dynamic visual stimuli, ameliorates upon entering adolescence (Spencer et al., 2000), which could point to an alleviation of a deficit in the temporal processing of sensory stimuli in ASD on an even more general level.

With respect to the maturation trajectories of PAC specifically, while the group difference in this study was driven by the youngest participants, this was not the case during the visual processing of faces. In a study focusing on upright faces, the group difference in PAC was driven by the oldest, not youngest, participants, with the same age range as here (Mamashli et al., 2018). In a follow-up study of the same cohort, we again found group differences in PAC during the processing of inverted faces (Mamashli et al., 2021), and this time without any correlation with age. A separate study on PAC during resting state in ASD that spanned up to age 16 also found no correlation between PAC and age in ASD (nor the control group) (Port et al., 2019). Together, these findings support the idea that differences in the maturation of PAC in ASD may be specific to task and brain region. As discussed above, the differences in PAC driven by the youngest participants observed here could indicate a delayed maturation of this process in ASD, rather than a permanent impairment. In contrast, it is known that face processing deficits continue well into adulthood in ASD (Dawson et al., 2005), and the increasing demands on face processing skills with age could potentially explain why PAC group differences in face processing are mostly driven by older participants. It is important to note that larger sample sizes, greater age spans, and ideally longitudinal studies would be needed to test the validity of the proposed ideas.

4.3. Limitations

The interpretation of our results needs to be considered in the context of the limitations of the study. First, we did not measure the perception or intelligibility of the present stimuli in our participants, but instead relied on prior literature to guide our design and interpretation (Carrell and Opie, 1992; Lewis and Carrell, 2007). It is possible that different participants would perceive the stimuli as having different degrees of speech-like quality and different levels of intelligibility if they were actively attending to the stimuli. Second, while the cortical location of the significant group difference in the local and long-range functional connectivity analysis is compatible with findings on the neural correlates of auditory object binding (Sohoglu et al., 2020; Yao et al., 2020), the location is more anterior than, for example, the one reported in Sohoglu et al. (2020), making it difficult to definitively dissociate the proposed object binding from effects of attention capture and switching (Cusack et al., 2010). However, while we cannot rule out the possibility of attentional differences contributing to the observed group difference, the nature of the employed passive paradigm together with the lack of any association of the connectivity measures with the behavioral ICSS or SCSS scores (measuring attentional inhibition and attentional switching, respectively) in part support our interpretation. It is also possible that the use of passive listening resulted in a different pattern of MEG responses and group effects than would have been obtained using an active task that requires attention to the stimuli and perceptual judgements. That said, temporal-coherence based binding of acoustic components is generally thought to occur in a bottom-up manner with attention thought to be allocated to bound objects rather than to individual acoustic cues (Shinn-Cunningham, 2008). Another potential limitation in our study is the lack of correlation of the connectivity measures with overall ASD severity. However, this concern is mitigated by findings showing that language development deficits do not covary strongly with autistic traits (Taylor et al., 2014). Such associations are likely to be more specific to the speech and communication impairments characteristic of ASD, rather than to ASD severity more broadly. Lastly, it should be noted that, as in many other studies involving neuroimaging and especially MRI, the ASD participants clustered around the upper end of the autism spectrum in terms of severity. Therefore, whether these findings would extend to ASD participants with more profound presentations, and in particular with more profoundly impacted auditory processing, is not known.

4.4. Conclusions

In summary, we found atypically increased feedforward functional connectivity from left primary auditory cortex to parietal cortex with concurrent decreased local functional connectivity within the left parietal cortical region when children with ASD were passively listening to speech stimuli that included bottom-up binding cues, compared to stimuli that did not. Considering the importance of temporal coherence

as a binding cue in natural sounds together with the proposed functional roles of the parietal cortex in auditory object binding and in time-dependent speech sequencing as part of the dorsal auditory stream, our findings imply a deficiency in the temporal processing of speech in ASD. More specifically, our results suggest both abnormally enhanced feedforward recruitment of the dorsal auditory stream and impaired binding of acoustic components of speech into a coherent perceptual stream based on temporal coherence in ASD. The atypical feedforward drive together with the correlation of the individual long-range functional connectivity measures with behavioral scores measuring auditory processing abnormalities imply that the proposed temporal processing impairment in ASD was likely driven by atypical sensory processing rather than top-down modulation by higher-order cognitive mechanisms. Lastly, the divergent maturational trajectories of the local functional connectivity between the groups, with the group differences driven largely by the youngest participants, suggests that the atypical speech binding in ASD might ameliorate with maturation.

CRediT authorship contribution statement

Jussi Alho: Conceptualization, Data curation, Formal analysis, Investigation, Software, Visualization, Writing – original draft. **Sheraz Khan:** Conceptualization, Investigation, Writing – review & editing. **Fahimeh Mamashli:** Investigation, Writing – review & editing. **Tyler K. Perrachione:** Conceptualization, Resources, Visualization, Writing – review & editing. **Ainsley Losh:** Investigation, Writing – review & editing. **Nicole McGuiggan:** Data curation, Investigation, Writing – review & editing. **Steven Graham:** Data curation, Investigation, Writing – review & editing. **Zein Nayal:** Data curation, Investigation, Writing – review & editing. **Robert M. Joseph:** Resources, Writing – review & editing. **Matti S. Hämäläinen:** Methodology, Writing – review & editing. **Hari Bharadwaj:** Conceptualization, Investigation, Resources, Supervision, Writing – original draft, Writing – review & editing. **Tal Kenet:** Conceptualization, Funding acquisition, Investigation, Project administration, Supervision, Writing – original draft, Writing – review & editing.

Declaration of Competing Interest

The authors declare that they have no known competing financial interests or personal relationships that could have appeared to influence the work reported in this paper.

Data availability

Data will be made available on request.

Acknowledgements

This work was supported by grants from the Nancy Lurie Marks Family Foundation (T.K), The Simons Foundation (SFARI 239395, T.K.), The National Institute of Child Health and Development (R01HD073254, T.K.), The National Institute of Mental Health (R01MH117998, R21MH116517, T.K.), National Institute of Deafness and Other Communication Disorders (R01DC015989, H.B.), Hearing Health Foundation (Emerging Research Grant, H.B.), National Institute for Biomedical Imaging and Bioengineering (P41EB01589 and P41EB030006, M.S.H.), National Institute of Neurological Disorders and Stroke (R01NS104585, M.S.H.), and a NARSAD Young Investigator grant from the Brain and Behavior Research Foundation (T.K.P.).

Appendix A. Supplementary data

Supplementary data to this article can be found online at https://doi.org/10.1016/j.nicl.2023.103336.

References

Alcántara, J.I., Weisblatt, E.J.L., Moore, B.C.J., Bolton, P.F., 2004. Speech-in-noise perception in high-functioning individuals with autism or Asperger's syndrome. J. Child Psychol. Psychiatry Allied Discip. 45 (6), 1107–1114.
Alho, J., Bharadwaj, H., Khan, S., Mamashli, F., Perrachione, T.K., Losh, A., McGuiggan, N.M., Joseph, R.M., Hämäläinen, M.S., Kenet, T., 2021. Altered maturation and atypical cortical processing of spoken sentences in autism spectrum disorder. Prog. Neurobiol. 203, 102077.
Amso, D., Haas, S., Tenenbaum, E., Markant, J., Sheinkopf, S.J., 2014. Bottom-up attention orienting in young children with autism. J. Autism Dev. Disord. 44 (3), 664–673.
Arnett, A.B., Hudac, C.M., DesChamps, T.D., Cairney, B.E., Gerdts, J., Wallace, A.S., Bernier, R.A., Webb, S.J., 2018. Auditory perception is associated with implicit language learning and receptive language ability in autism spectrum disorder. Brain Lang. 187, 1–8.
Ben-Sasson, A., Hen, L., Fluss, R., Cermak, S.A., Engel-Yeger, B., Gal, E., 2009. A meta-analysis of sensory modulation symptoms in individuals with autism spectrum disorders. J. Autism Dev. Disord. 39 (1), 1–11.
Bharadwaj, H., Mamashli, F., Khan, S., Singh, R., Joseph, R.M., Losh, A., Pawlyszyn, S., McGuiggan, N.M., Graham, S., Hämäläinen, M.S., Kenet, T., Griffiths, T.D., 2022. Cortical signatures of auditory object binding in children with autism spectrum disorder are anomalous in concordance with behavior and diagnosis. PLOS Biol. 20 (2), e3001541.
Bizley, J.K., Cohen, Y.E., 2013. The what, where and how of auditory-object perception. Nat. Rev. Neurosci. 14, 693–707. https://doi.org/10.1038/nrn3565.
Bloy, L., Shwayder, K., Blaskey, L., Roberts, T.P.L., Embick, D., 2019. A Spectrotemporal Correlate of Language Impairment in Autism Spectrum Disorder. J. Autism Dev. Disord. 49 (8), 3181–3190.
Bonnel, A., Mottron, L., Peretz, I., Trudel, M., Gallun, E., Bonnel, A.-M., 2003. Enhanced pitch sensitivity in individuals with autism: A signal detection analysis. J. Cogn. Neurosci. 15 (2), 226–235.
Bornkessel-Schlesewsky, I., Schlesewsky, M., 2013. Reconciling time, space and function: A new dorsal-ventral stream model of sentence comprehension. Brain Lang. 125, 60–76. https://doi.org/10.1016/j.bandl.2013.01.010.
Braddick, O., Atkinson, J., Wattam-Bell, J., 2003. Normal and anomalous development of visual motion processing: Motion coherence and "dorsal-stream vulnerability". Neuropsychologia 41 (13), 1769–1784.
Brauer, J., Anwander, A., Perani, D., Friederici, A.D., 2013. Dorsal and ventral pathways in language development. Brain Lang. 127 (2), 289–295.
Bregman, A.S., 1994. Auditory scene analysis: The perceptual organization of sound. MIT press.
Brock, JON, Brown, C.C., Boucher, JILL, Rippon, GINA, 2002. The temporal binding deficit hypothesis of autism. Dev. Psychopathol. 14 (2), 209–224.
Brown, C., Dunn, W., 2002. Adolescent/adult sensory profile. San Antonio, TX.
Canolty, R.T., Knight, R.T., 2010. The functional role of cross-frequency coupling. Trends Cogn. Sci. 14 (11), 506–515.
Carrell, T.D., Opie, J.M., 1992. The effect of amplitude comodulation on auditory object formation in sentence perception. Percept. Psychophys. 52 (4), 437–445.
Changeux, J.-P., Danchin, A., 1976. Selective stabilisation of developing synapses as a mechanism for the specification of neuronal networks. Nature 264 (5588), 705–712.
Constantino, J.N., Gruber, C.P., 2012. Social responsiveness scale: SRS-2, second ed. Torrance, CA.
Cusack, R., Mitchell, D.J., Duncan, J., 2010. Discrete object representation, attention switching, and task difficulty in the parietal lobe. J. Cogn. Neurosci. 22 (1), 32–47.
Dale, A.M., Liu, A.K., Fischl, B.R., Buckner, R.L., Belliveau, J.W., Lewine, J.D., Halgren, E., 2000. Dynamic statistical parametric mapping: Combining fMRI and MEG for high-resolution imaging of cortical activity. Neuron 26 (1), 55–67.
Darwin, C.J., 1997. Auditory grouping. Trends Cogn. Sci. 1 (9), 327–333.
Davis, M.H., Johnsrude, I.S., 2007. Hearing speech sounds: Top-down influences on the interface between audition and speech perception. Hear. Res. 229, 132–147. https://doi.org/10.1016/j.heares.2007.01.014.
Dawson, G., Webb, S.J., McPartland, J., 2005. Understanding the nature of face processing impairment in autism: Insights from behavioral and electrophysiological studies. Dev. Neuropsychol. 27 (3), 403–424.
Desikan, R.S., Ségonne, F., Fischl, B., Quinn, B.T., Dickerson, B.C., Blacker, D., Buckner, R.L., Dale, A.M., Maguire, R.P., Hyman, B.T., Albert, M.S., Killiany, R.J., 2006. An automated labeling system for subdividing the human cerebral cortex on MRI scans into gyral based regions of interest. Neuroimage 31 (3), 968–980.
Dhamala, M., Rangarajan, G., Ding, M., 2008a. Estimating granger causality from fourier and wavelet transforms of time series data. Phys. Rev. Lett. 100 https://doi.org/10.1103/PhysRevLett.100.018701.
Dhamala, M., Rangarajan, G., Ding, M., 2008b. Analyzing information flow in brain networks with nonparametric Granger causality. Neuroimage 41 (2), 354–362.
Dupré la Tour, T., Tallot, L., Grabot, L., Doyère, V., van Wassenhove, V., Grenier, Y., Gramfort, A., Battaglia, F.P., 2017. Non-linear auto-regressive models for cross-frequency coupling in neural time series. PLoS Comput. Biol. 13 (12), e1005893.
Edgar, J.C., Fisk C.L. IV, Berman, J.I., Chudnovskaya, D., Liu, S., Pandey, J., Herrington, J.D., Port, R.G., Schultz, R.T., Roberts, T.P.L., 2015. Auditory encoding abnormalities in children with autism spectrum disorder suggest delayed development of auditory cortex. Mol. Autism. 6 (69) https://doi.org/10.1186/s13229-015-0065-5.
Elliot, C.D., 2007. Differential Ability Scales-II (DAS-II). San Antonio, TX.
Ellis, D.P.W., 2004. Sinewave Speech Analysis/Synthesis in Matlab. http://www.ee.columbia.edu/ln/labrosa/matlab/sws/.

Fischl, B., Sereno, M.I., Tootell, R.B.H., Dale, A.M., 1999. High-resolution intersubject averaging and a coordinate system for the cortical surface. Hum. Brain Mapp. 8 https://doi.org/10.1002/(SICI)1097-0193(1999)8:4<272::AID-HBM10>3.0.CO;2-4.

Foxe, J.J., Molholm, S., Del Bene, V.A., Frey, H.-P., Russo, N.N., Blanco, D., Saint-Amour, D., Ross, L.A., 2015. Severe multisensory speech integration deficits in high-functioning school-aged children with autism spectrum disorder (ASD) and their resolution during early adolescence. Cereb. Cortex 25 (2), 298–312.

Fries, P., 2005. A mechanism for cognitive dynamics: Neuronal communication through neuronal coherence. Trends Cogn. Sci. 9 (10), 474–480.

Giraud, A.-L., Poeppel, D., 2012. Cortical oscillations and speech processing: emerging computational principles and operations. Nat. Neurosci. 15, 511–517. https://doi.org/10.1038/nn.3063.

Gramfort, A., Luessi, M., Larson, E., Engemann, D.A., Strohmeier, D., Brodbeck, C., Goj, R., Jas, M., Brooks, T., Parkkonen, L., Hämäläinen, M., 2013. MEG and EEG data analysis with MNE-Python. Front. Neurosci. https://doi.org/10.3389/fnins.2013.00267.

Grinter, E.J., Maybery, M.T., Badcock, D.R., 2010. Vision in developmental disorders: Is there a dorsal stream deficit? Brain Res. Bull. 82 (3-4), 147–160.

Hämäläinen, M.S., Ilmoniemi, R.J., 1994. Interpreting magnetic fields of the brain: minimum norm estimates. Med. Biol. Eng. Comput. 32 (1), 35–42.

Hämäläinen, M.S., Sarvas, J., 1987. Feasibility of the homogeneous head model in the interpretation of neuromagnetic fields. Phys. Med. Biol. 32 (1), 91–97.

Hickok, G., Poeppel, D., 2007. The cortical organization of speech processing. Nat. Rev. Neurosci. 8, 393–402. https://doi.org/10.1038/nrn2113.

Howlin, P., Goode, S., Hutton, J., Rutter, M., 2004. Adult outcome for children with autism. J. Child Psychol. Psychiatry Allied Discip. 45 (2), 212–229.

Hull, C., Scanziani, M., 2007. It's about time for thalamocortical circuits. Nat. Neurosci. 10 (4), 400–402.

Hyvärinen, A., 1999. Fast and robust fixed-point algorithms for independent component analysis IEEE Trans. Neural Networks 10 (3), 626–634.

IEEE, 1969. IEEE Recommended Practice for Speech Quality Measurements. IEEE Trans. Audio Electroacoust. 17, 225–226. https://doi.org/10.1109/TAU.1969.1162058.

Järvinen-Pasley, A., Wallace, G.L., Ramus, F., Happé, F., Heaton, P., 2008. Enhanced perceptual processing of speech in autism. Dev. Sci. 11 (1), 109–121.

Kaas, J.H., Hackett, T.A., 2000. Subdivisions of auditory cortex and processing streams in primates. Proc. Natl. Acad. Sci. U. S. A. 97 (22), 11793–11799.

Kana, R.K., Libero, L.E., Moore, M.S., 2011. Disrupted cortical connectivity theory as an explanatory model for autism spectrum disorders. Physics of Life Reviews 8 (4), 410–437.

Kana, R.K., Uddin, L.Q., Kenet, T., Chugani, D., Müller, R.-A., 2014. Brain connectivity in autism. Front. Hum. Neurosci. 8, 349.

Kaufman, A.S., 2004. Kaufman brief intelligence test, second ed. Pines, MN.

Khan, S., Gramfort, A., Shetty, N.R., Kitzbichler, M.G., Ganesan, S., Moran, J.M., Lee, S. M., Gabrieli, J.D.E., Tager-Flusberg, H.B., Joseph, R.M., Herbert, M.R., Hämäläinen, M.S., Kenet, T., 2013. Local and long-range functional connectivity is reduced in concert in autism spectrum disorders. Proc. Natl. Acad. Sci. U. S. A. 110 (8), 3107–3112.

Khan, S., Michmizos, K., Tommerdahl, M., Ganesan, S., Kitzbichler, M.G., Zetino, M., Garel, K.-L., Herbert, M.R., Hämäläinen, M.S., Kenet, T., 2015. Somatosensory cortex functional connectivity abnormalities in autism show opposite trends, depending on direction and spatial scale. Brain 138 (5), 1394–1409.

Kitzbichler, M.G., Khan, S., Ganesan, S., Vangel, M.G., Herbert, M.R., Hämäläinen, M.S., Kenet, T., 2015. Altered development and multifaceted band-specific abnormalities of resting state networks in autism. Biol. Psychiatry. 77 (9), 794–804.

Kramer, M.A., Tort, A.B.L., Kopell, N.J., 2008. Sharp edge artifacts and spurious coupling in EEG frequency comodulation measures. J. Neurosci. Methods 170 (2), 352–357.

Kwakye, L.D., Foss-Feig, J.H., Cascio, C.J., Stone, W.L., Wallace, M.T., 2011. Altered auditory and multisensory temporal processing in autism spectrum disorders. Front. Integr. Neurosci. https://doi.org/10.3389/fnint.2010.00129.

Lee, Y., Park, B.Y., James, O., Kim, S.G., Park, H., 2017. Autism spectrum disorder related functional connectivity changes in the language network in children, adolescents and adults. Front. Hum. Neurosci. 11 https://doi.org/10.3389/fnhum.2017.00418.

Lewis, D.E., Carrell, T.D., 2007. The effect of amplitude modulation on intelligibility of time-varying sinusoidal speech in children and adults. Percept. Psychophys. 69 (7), 1140–1151.

Lin, F.-H., Witzel, T., Ahlfors, S.P., Stufflebeam, S.M., Belliveau, J.W., Hämäläinen, M.S., 2006. Assessing and improving the spatial accuracy in MEG source localization by depth-weighted minimum-norm estimates. Neuroimage 31 (1), 160–171.

Lombardo, M., Pierce, K., Eyler, L., Carter, C., Barnes, Ahrens-Barbeau, C., Solso, S., Campbell, K., Courchesne, E., 2015. Different functional neural substrates for good and poor language outcome in autism. Neuron 86 (2), 567–577.

Lord, C., Risi, S., Lambrecht, L., Cook, E.H., Leventhal, B.L., Dilavore, P.C., Pickles, A., Rutter, M., 2000. The Autism Diagnostic Observation Schedule-Generic: A standard measure of social and communication deficits associated with the spectrum of autism. J. Autism Dev. Disord. 30, 205-223. https://doi.org/10.1023/A:1005592401947.

Magiati, I., Tay, X.W., Howlin, P., 2014. Cognitive, language, social and behavioural outcomes in adults with autism spectrum disorders: A systematic review of longitudinal follow-up studies in adulthood. Clin. Psychol. Rev. 34 (1), 73–86.

Mamashli, F., Khan, S., Bharadwaj, H., Michmizos, K., Ganesan, S., Garel, K.-L., Ali Hashmi, J., Herbert, M.R., Hämäläinen, M., Kenet, T., 2017. Auditory processing in noise is associated with complex patterns of disrupted functional connectivity in autism spectrum disorder. Autism Res. 10 (4), 631–647.

Mamashli, F., Khan, S., Bharadwaj, H., Losh, A., Pawlyszyn, S.M., Hämäläinen, M.S., Kenet, T., 2018. Maturational trajectories of local and long-range functional connectivity in autism during face processing. Hum. Brain Mapp. 39 (10), 4094–4104.

Mamashli, F., Kozhemiako, N., Khan, S., Nunes, A.S., McGuiggan, N.M., Losh, A., Joseph, R.M., Ahveninen, J., Doesburg, S.M., Hämäläinen, M.S., Kenet, T., 2021. Children with autism spectrum disorder show altered functional connectivity and abnormal maturation trajectories in response to inverted faces. Autism Res. 14 (6), 1101–1114.

Maris, E., Oostenveld, R., 2007. Nonparametric statistical testing of EEG- and MEG-data. J. Neurosci. Methods 164, 177–190. https://doi.org/10.1016/j.jneumeth.2007.03.024.

McCormick, C., Hepburn, S., Young, G.S., Rogers, S.J., 2016. Sensory symptoms in children with autism spectrum disorder, other developmental disorders and typical development: A longitudinal study. Autism 20 (5), 572–579.

Nomi, J.S., Uddin, L.Q., 2015. Developmental changes in large-scale network connectivity in autism. NeuroImage Clin. 7, 732–741.

O'Connor, K., 2012. Auditory processing in autism spectrum disorder: A review. Neurosci. Biobehav. Rev. 36 (2), 836–854.

O'Reilly, C., Lewis, J.D., Elsabbagh, M., Gozzi, A., 2017. Is functional brain connectivity atypical in autism? A systematic review of EEG and MEG studies. PLoS One 12 (5), e0175870.

Oostenveld, R., Fries, P., Maris, E., Schoffelen, J.-M., 2011. FieldTrip: Open source software for advanced analysis of MEG, EEG, and invasive electrophysiological data. Comput. Intell. Neurosci. 2011, 1–9.

Oram Cardy, J.E., Flagg, E.J., Roberts, W., Roberts, T.P.L., 2005. Delayed mismatch field for speech and non-speech sounds in children with autism. Neuroreport 16 (5), 521–525.

Özkurt, T.E., Schnitzler, A., 2011. A critical note on the definition of phase-amplitude cross-frequency coupling. J. Neurosci. Methods 201 (2), 438–443.

Pellicano, E., Gibson, L., Maybery, M., Durkin, K., Badcock, D.R., 2005. Abnormal global processing along the dorsal visual pathway in autism: A possible mechanism for weak visuospatial coherence? Neuropsychologia 43 (7), 1044–1053.

Perrachione, T.K., Dougherty, S.C., Mclaughlin, D.E., Lember, R.A., 2015. The effects of speech perception and speech comprehension on talker identification. In: Proceedings of the 18th International Congress of Phonetic Sciences.

Piro, J.M., 1998. Handedness and intelligence: Patterns of hand preference in gifted and nongifted children. Dev. Neuropsychol. 14 (4), 619–630.

Port, R.G., Edgar, J.C., Ku, M., Bloy, L., Murray, R., Blaskey, L., Levy, S.E., Roberts, T.P. L., 2016. Maturation of auditory neural processes in autism spectrum disorder - A longitudinal MEG study. NeuroImage Clin 11, 566–577.

Port, R.G., Dipiero, M.A., Ku, M., Liu, S., Blaskey, L., Kuschner, E.S., Edgar, J.C., Roberts, T.P.L., Berman, J.I., 2019. Children with Autism Spectrum Disorder Demonstrate Regionally Specific Altered Resting-State Phase-Amplitude Coupling. Brain Connect. 9 (5), 425–436.

Rauschecker, J.P., 1997. Processing of Complex Sounds in the Auditory Cortex of Cat, Monkey, and Man. Acta Oto-Laryngologica 117 (sup532), 34–38.

Rauschecker, J.P., 2011. An expanded role for the dorsal auditory pathway in sensorimotor control and integration. Hear. Res. 271, 16–25. https://doi.org/10.1016/j.heares.2010.09.001.

Rauschecker, J.P., Scott, S.K., 2009. Maps and streams in the auditory cortex: nonhuman primates illuminate human speech processing. Nat. Neurosci. 12, 718–724. https://doi.org/10.1038/nn.2331.

Rauschecker, J.P., Tian, B., 2000. Mechanisms and streams for processing of "what" and "where" in auditory cortex. Proc. Natl. Acad. Sci. U. S. A. 97 (22), 11800–11806.

Remez, R.E., Rubin, P.E., Pisoni, D.B., Carrell, T.D., 1981. Speech perception without traditional speech cues. Science 212 (4497), 947–950.

Risi, S., Lord, C., Gotham, K., Corsello, C., Chrysler, C., Szatmari, P., Cook, E.H., Leventhal, B.L., Pickles, A., 2006. Combining information from multiple sources in the diagnosis of autism spectrum disorders. J. Am. Acad. Child Adolesc. Psychiatry 45 (9), 1094–1103.

Roberts, T.P.L., Khan, S.Y., Rey, M., Monroe, J.F., Cannon, K., Blaskey, L., Woldoff, S., Qasmieh, S., Gandal, M., Schmidt, G.L., Zarnow, D.M., Levy, S.E., Edgar, J.C., 2010. MEG detection of delayed auditory evoked responses in autism spectrum disorders: Towards an imaging biomarker for autism. Autism Res. 3 (1), 8–18.

Roberts, T.P.L., Cannon, K.M., Tavabi, K., Blaskey, L., Khan, S.Y., Monroe, J.F., Qasmieh, S., Levy, S.E., Edgar, J.C., 2011. Auditory magnetic mismatch field latency: A biomarker for language impairment in autism. Biol. Psychiatry. 70 (3), 263–269.

Robertson, C.E., Baron-Cohen, S., 2017. Sensory perception in autism. Nat. Rev. Neurosci. 18 (11), 671–684.

Robertson, C.E., Thomas, C., Kravitz, D.J., Wallace, G.L., Baron-Cohen, S., Martin, A., Baker, C.I., 2014. Global motion perception deficits in autism are reflected as early as primary visual cortex. Brain 137 (9), 2588–2599.

Rosen, S., 1992. Temporal information in speech: acoustic, auditory and linguistic aspects. Trans. R. Soc. Lond. B. Biol. Sci Philos. 336, 367–373. https://doi.org/10.1098/rstb.1992.0070.

Seymour, R.A., Rippon, G., Gooding-Williams, G., Schoffelen, J.M., Kessler, K., 2019. Dysregulated oscillatory connectivity in the visual system in autism spectrum disorder. Brain 142 (10), 3294–3305.

Shamma, S.A., Elhilali, M., Micheyl, C., 2011. Temporal coherence and attention in auditory scene analysis. Trends Neurosci 34 (3), 114–123.

Shinn-Cunningham, B.G., 2008. Object-based auditory and visual attention. Trends Cogn. Sci. 12 (5), 182–186.

Sohoglu, E., Kumar, S., Chait, M., Griffiths, T.D., 2020. Multivoxel codes for representing and integrating acoustic features in human cortex. Neuroimage 217, 116661.

Spencer, J., O'Brien, J., Riggs, K., Braddick, O., Atkinson, J., Wattam-Bell, J., 2000. Motion processing in autism: Evidence for a dorsal stream deficiency. Neuroreport 11 (12), 2765–2767.
Stephen, J.M., Hill, D.E., Peters, A., Flynn, L., Zhang, T., Okada, Y., 2017. Development of Auditory Evoked Responses in Normally Developing Preschool Children and Children with Autism Spectrum Disorder. Dev. Neurosci. 39 (5), 430–441.
Taulu, S., Kajola, M., 2005. Presentation of electromagnetic multichannel data: The signal space separation method. J. Appl. Phys. doi 10 (1063/1), 1935742.
Taulu, S., Simola, J., 2006. Spatiotemporal signal space separation method for rejecting nearby interference in MEG measurements. Phys. Med. Biol. 51 (7), 1759–1768.
Taylor, M.J., Charman, T., Robinson, E.B., Hayiou-Thomas, M.E., Happé, F., Dale, P.S., Ronald, A., 2014. Language and traits of autism spectrum conditions: Evidence of limited phenotypic and etiological overlap. Am. J. Med. Genet. Part B Neuropsychiatr. Genet. 165 (7), 587–595.
Taylor, N., Isaac, C., Milne, E., 2010. A comparison of the development of audiovisual integration in children with autism spectrum disorders and typically developing children. J. Autism Dev. Disord. 40 (11), 1403–1411.
Tomchek, S.D., Dunn, W., 2007. Sensory processing in children with and without autism: a comparative study using the short sensory profile. Am. J. Occup. Ther. 61 (2), 190–200.
Uutela, K., Taulu, S., Hämäläinen, M., 2001. Detecting and correcting for head movements in neuromagnetic measurements. Neuroimage 14 (6), 1424–1431.
Van der Hallen, R., Evers, K., Brewaeys, K., Van den Noortgate, W., Wagemans, J., 2015. Global processing takes time: A meta-analysis on local-global visual processing in ASD. Psychol. Bull. 141 (3), 549–573.
Vinck, M., Oostenveld, R., Van, M., Wingerden, Battaglia, F., Pennartz, C.M., a,, 2011. An improved index of phase-synchronization for electrophysiological data in the presence of volume-conduction, noise and sample-size bias. Neuroimage 55, 1548–1565. https://doi.org/10.1016/j.neuroimage.2011.01.055.
Yao, J.D., Gimoto, J., Constantinople, C.M., Sanes, D.H., 2020. Parietal Cortex Is Required for the Integration of Acoustic Evidence. Curr. Biol. 30 (17), 3293–3303.e4.
Zhang, J., Evans, A., Hermoye, L., Lee, S.K., Wakana, S., Zhang, W., Donohue, P., Miller, M.I., Huang, H., Wang, X., van Zijl, P.C.M., Mori, S., 2007. Evidence of slow maturation of the superior longitudinal fasciculus in early childhood by diffusion tensor imaging. Neuroimage 38. https://doi.org/10.1016/j.neuroimage.2007.07.033.